

Entanglement in a dephasing model and many-body localization

Marko Žnidarič

*Physics Department, Faculty of Mathematics and Physics,
University of Ljubljana, 1000 Ljubljana, Slovenia*

(Dated: August 20, 2022)

We study entanglement dynamics in a diagonal dephasing model in which the strength of interaction decays exponentially with distance – the so-called l-bit model of many-body localization. We calculate the exact expression for entanglement growth with time, finding in addition to a logarithmic growth, a sub-logarithmic correction. Provided the l-bit picture correctly describes the many-body localized phase this implies that the entanglement in such systems does not grow (just) as a logarithm of time, as believed so far.

I. INTRODUCTION

Localization is a phenomenon that, due to its peculiar properties, is of interest in different fields of physics. As its name already implies, one of the characteristic properties is a lack of transport and as such it was first considered within solid-state questions of transport. Somewhat surprisingly Anderson found [1] that in one-dimension and for noninteracting particles an infinitesimal disorder causes an abrupt change of all eigenstates from extended to localized. Being an interference phenomenon one could argue that any interaction between particles will wash out precise phase relations and thereby destroy localization. That this needs not be so was shown using diagrammatics in Ref. [2], see also [3]. A couple of numerical works followed [4, 5], realizing that such many-body localized (MBL) systems display many interesting properties [6, 7]. This eventually led to a flurry of activity in recent years, see Ref. [8] for a review.

One of the characteristic features of MBL systems is its logarithmic in time growth of entanglement entropy [5] (in a finite system the entropy growth will eventually stop at a volume-law saturation value [9]). Although conserved quantities like energy or particles are not transported in MBL systems, quantum (information) correlations do spread, which is in contrast to a single-particle (i.e., Anderson) localization where the entropy does not grow. Logarithmic growth has been explained early on as being caused by a dephasing due to exponentially decaying effective interaction [10, 11], see also Ref. [12], with a prefactor that is equal to the localization length [10, 12–15]. This picture has been furthermore elaborated by a so-called l-bit picture [13, 14] that nowadays constitutes what is believed to be the fullest description of MBL. It relies on an existence of a (quasi) local integrals of motion such that a quasi-local unitary transformation can change an MBL hamiltonian from its physical basis (real space) to a logical l-bit basis where H is diagonal, and can be written as,

$$H = \sum_k J_k^{(1)} \sigma_k^z + \sum_{k < l} J_{k,l}^{(2)} \sigma_k^z \sigma_l^z + \sum_{k < l < m} J_{k,l,m}^{(3)} \sigma_k^z \sigma_l^z \sigma_m^z + \dots, \quad (1)$$

with σ_k^z being the Pauli matrix at the k -th l-bit site. Because it is diagonal the l-bit hamiltonian (1) manifestly

displays the emergent effective integrability of MBL systems [16, 17], another reason for their high interest. While for most systems that are believed to be MBL the existence of the l-bit description is in principle a conjecture, its construction is implicit in a proof of MBL for a particular system [18]. It is also able to describe many phenomenological properties of MBL systems [19] and is as such widely believed to be the correct description of MBL.

Still, considering a vast amount of predominantly numerical works (see though e.g. Refs. [18, 20, 21] for exact results) discussing MBL in general, as well as entanglement specifically, e.g. being at a core of a definition of MBL [22], its behavior in the MBL phase or close to the transition [11, 23–30], in long-range [31, 32] and time-dependent [33] systems, or for bond disorder [34], it would be extremely useful to have analytical results for MBL systems. Our goal is to provide such a result for entanglement growth. We study the dynamics of entanglement in a diagonal l-bit model, which will then in turn give tight bounds on the growth of entanglement in the original physical basis. Considering its widespread use and a “well established” logarithmic growth, we surprisingly find that it is in fact not just logarithmic but has instead a subleading correction.

In Sec. II. we specify a random l-bit model with exponentially decaying interaction between any pair of spins and discuss saturation value of entanglement at long times. In Sec. III. we solve the model and calculate the explicit time dependence of the Reny-2 entropy (purity). This section gives our main result – the entropy growth is not just logarithmic in time. While the exact result is for a particular initial state, we argue and numerically demonstrate that our result is robust with respect to different generic initial states, distribution of couplings, and other Reny entropies. In Sec. IV. we then discuss the 3-body model, again getting similar result. In Sec. V. we explain how the result for the l-bit model directly translate to MBL systems in the physical basis at long times. Finally, in Sec. VI. we numerically study time evolution of individual eigenvalues, fully specifying the entanglement content of an evolved state.

II. THE 2-BODY RANDOM MODEL

The local integrals of motion model, or short the 1-bit model, is given by a diagonal hamiltonian in Eq.(1) where one assumes that $J_{k,l,\dots}^{(r)}$ decay exponentially with increasing maximal distance between their site indices k, l, \dots , as well as with the increasing order r [13, 14]. System length is L , Hilbert space size $N = 2^L$, while k, l, m will be site indices. Most of the time we shall focus on a random 2-body model for which $J^{(r)} \equiv 0$ for all $r > 2$, while $J_k^{(1)}$ and $J_{k,l}^{(2)}$ are independent random numbers. Such model is simpler for analytical treatment while, as we will argue, still retains all the features of the full model (1). We want to describe time evolution with such H .

At first sight the problem might appear trivial – after all H is diagonal with eigenstates being just the basis (computational) states. While the evolution is indeed trivial (no evolution) if one starts with a single basis state (in the 1-bit basis), situation can be rather complex if one starts with a *superposition* of basis states (even if they represent a product state). Complexity in quantum mechanics can come not just from the dynamics but also from the complexity of an initial state. One can in fact ask what is the complexity of simulating evolution by diagonal matrices, in other words of the dynamics governed only by phases (commuting operators). The answer is not known, though it is believed [35] that such circuits in general can not be simulated efficiently on a classical computer. MBL systems are in this sense not generic as their entanglement grows logarithmically with time [36], and thus the simulation complexity polynomially with time (low entanglement is a sufficient, but not necessary, condition for an efficient simulability).

Starting from a pure state $|\psi(0)\rangle = \sum_{p=1}^N c_p |p\rangle$ we would like to calculate the entanglement in a state after time t , $|\psi(t)\rangle = e^{-iHt}|\psi(0)\rangle$. For pure states the bipartite entanglement is fully specified by the spectrum of the reduced density matrix $\rho_A(t) = \text{tr}_B|\psi(t)\rangle\langle\psi(t)|$. A convenient measure is purity, $I(t) = \text{tr}\rho_A^2$, and closely related Reny-2 entropy $S_2(t) := -\log_2 I(t)$. In all our calculations we shall calculate the average $I(t)$ and then take its logarithm to get $S_2(t)$, arguing that $S_2(t)$ for large times and in the thermodynamic limit (TDL) behaves essentially the same as any other Reny entropy, including the von Neumann entropy, and furthermore, due to self-averaging taking the logarithm of the average is essentially the same as taking the average of the logarithm. While the eigenstates of H are simple the eigenenergies are combinations of various $J_{j,k,\dots}^{(r)}$, depending on the orientations of individual spins. Let us denote those eigenstate by $E_{j\alpha}$, where we shall use a double (multi)index labeling bipartite eigenstates $|\mathbf{j}\rangle_A \otimes |\alpha\rangle_B$ (we use i, j, α, β as eigenstate (multi)indices, dropping from now on the vectorial notation on them). Calculating purity one gets

$$I(t) = \sum_{i,j,\alpha,\beta} c_{i\alpha} c_{j\alpha}^* c_{i\beta} c_{j\beta}^* e^{-i(E_{i\alpha} - E_{j\alpha} + E_{j\beta} - E_{i\alpha})t}. \quad (2)$$

A. Saturation value

First, few comments about the asymptotic saturation value of $I(t \rightarrow \infty)$. Assuming the eigenenergies are ergodic (which is the case for our 2-body model), performing an infinite time averaging one has $\overline{\exp(-i(E_{i\alpha} - E_{j\alpha} + E_{j\beta} - E_{i\alpha})t)} = \delta_{ij} + \delta_{\alpha\beta} - \delta_{ij}\delta_{\alpha\beta}$, resulting in $\overline{I(t)} = \sum_{i,\alpha,\beta} |c_{i\alpha}|^2 |c_{i\beta}|^2 + \sum_{i,j,\alpha} |c_{i\alpha}|^2 |c_{j\alpha}|^2 - \sum_{i,\alpha} |c_{i\alpha}|^4$ (similar calculations have been used many times [42, 43]). Taking an initial product state $|\psi(0)\rangle = (\cos \frac{\varphi}{2}|0\rangle + \sin \frac{\varphi}{2}|1\rangle)^{\otimes L}$ gives a saturation value of purity for a bipartition into $L_A = L - L_B$ consecutive sites $\overline{I(t)} = q^{L_A} + q^{L_B} - q^L$, where $q := \frac{3+\cos 2\varphi}{4} = \frac{1+z^2}{2}$, and $z := \langle\psi(0)|\sigma_j^z|\psi(0)\rangle$. Focusing on an equal bipartition, $L_A = \frac{L}{2}$, the expression for the saturation value of S_2 simplifies to $\overline{S_2(t)} = c \frac{L}{2} - 1$, with $c := \log_2 \frac{2}{1+z^2}$. The saturation value of the entropy therefore always satisfies a volume law, with a prefactor c being the larger the smaller is the value of the initial z (formula for $c(z)$ explains numerical observation in Ref.[15]). From an experimental (real or numerical) point of view it is therefore the best to choose an initial state with $z = 0$ – this will result in the largest saturation value and therefore the largest range of values where the entropy growth can be observed. With that aim we shall focus on the initial state with $\varphi = \frac{\pi}{2}$ ($z = 0$), i.e., $c_{j\alpha} = 1/\sqrt{N}$ (later we shall show that random product initial states give the same behavior).

III. TIME EVOLUTION

Let us now return to our main focus – the time dependence of $I(t)$. Using $c_{j\alpha} = 1/\sqrt{N}$ Eq. (2) simplifies for the 2-body model to

$$I(t) = \frac{1}{N^2} \sum_{i,j \in A, \alpha, \beta \in B} e^{-it(\mathbf{z}_i - \mathbf{z}_j) \cdot J_{AB}^{(2)} \cdot (\mathbf{z}_\alpha - \mathbf{z}_\beta)}, \quad (3)$$

where $\mathbf{z}_i = (z_{i1}, z_{i2}, \dots, z_{iL_A})$ is a vector denoting spin orientation $z_{ik} \in \{+1, -1\}$ in an eigenstate labeled by a multiindex i . Purity depends only on the terms in H that directly couple spins in A and B and are contained in a matrix $J_{AB}^{(2)}$ containing 2-body coupling constants, and is of size $L_A \times L_B$. 1-body terms $J_k^{(1)}$ cancel out. Eq. (3) is the central formula that we build upon. For a Gaussian distribution of $J_{k,l}^{(2)}$, $p(x = J_{k,k+r}^{(2)}) \sim e^{-x^2/2J^2W_r^2}$, with the variance $\langle J_{k,k+r}^{(2)} \rangle = J^2W_r^2 := J^2e^{-2(r-1)/\xi}$. The size of the coupling decays exponentially with distance, the decay length being ξ , while J sets the energy (time) scale.

We are predominantly interested in the long-time behavior when the entanglement is large (volume law that is a (small) fraction of $\sim L$) and the states involved are thus generic. Therefore one expects that relative sample-to-sample fluctuations decrease with time and can be neglected. Averaging purity (3) over Gaussian distribution of couplings one gets the average purity,

$$\langle I(t) \rangle = \frac{1}{N} \sum_{i,\alpha} \prod_{k \in A, l \in B} e^{-8J^2 t^2 W_{l-k}^2 \delta_{z_{i_k},1} \delta_{z_{\alpha_l},1}}. \quad (4)$$

For a non-Gaussian distribution of $J^{(2)}$ one would have in Eq.(4) instead a product of Fourier transformations of

the distribution $p(x)$. Essentials would be the same (see Appendix A). While the expression (4) is simpler than (3), being a sum of N instead of N^2 terms, it is still combinatorially complex. In the sum over 2^L bit strings $|i, \alpha\rangle$ each pair of bits k, l (from parts A and B, respectively) contributes a term $\sim W_{l-k}^2$ in the exponential argument if the k -th and l -th bits are $+1$. While many of N bit strings result in the same argument of the exponential, there are still of order $\approx 0.4N$ different terms and the expression can not be much more simplified provided one wants to retain its exactness.

To give an idea of the form that $\langle I(t) \rangle$ takes we write the exact expression for $L = 4$ and $L_A = 2$,

$$\langle I(t) \rangle = \frac{1}{16} \left[7 + \left(e^{-\tau^2 W_1^2} + 2e^{-\tau^2 (W_1^2 + W_2^2)} + e^{-\tau^2 (W_1^2 + 2W_2^2 + W_3^2)} \right) + \left(2e^{-\tau^2 W_2^2} + 2e^{-\tau^2 (W_2^2 + W_3^2)} \right) + \left(e^{-\tau^2 W_3^2} \right) \right], \quad (5)$$

where $\tau^2 := 8J^2 t^2$. Round brackets group terms whose leading argument is W_r^2 , $r = 0, 1, 2, 3$. We have generated such exact expressions for an equal bipartitions for up to $L = 34$ spins (where $\langle I(t) \rangle$ is a sum of the order of $\sim 10^{10}$ exponential functions with different arguments). While they are obviously too long to be written out, their general form is

$$\langle I(t) \rangle = \frac{1}{N} \left[\left(2^{1+\frac{L}{2}} - 1 \right) + \sum_{r=1}^{L-1} \sum_m d_m^{(r)} e^{-\tau^2 \sum_{p=r}^{L-1} c_{m,p}^{(r)} W_p^2} \right]. \quad (6)$$

The first constant term is just the saturation value giving the already mentioned $-\log_2 \langle I(t) \rangle = \frac{L}{2} - 1 - \log_2 (1 - 2^{-L/2-1})$. One can show that the leading coefficient is $c_{m,r}^{(r)} = 1$ for all r (also, trivially, $c_{m,p}^{(r)} \leq p$, because there can be at most p links of length p across a given cut).

A. Small localization length

Let us first discuss the case of small ξ where analytic treatment is the simplest, the physics is transparent and at the same time similar to the one for larger ξ . Because W_r^2 decrease exponentially with r we can in each of N terms in Eq.(4) retain in the argument only terms with the smallest r in $W_{r=l-k}^2$ (we can do that because $c_{m,p}^{(r)}$ grow at most linearly with p), see also the explicit example in Eq. (5). The number of such terms, denoted by $a_r := \sum_m d_m^{(r)}$, can be calculated exactly. Looking at (4) we have to consider contributions from 2^L possible bit strings of length L . If we are interested in terms that have a minimal distance r (i.e., leading order W_r^2) it is enough to consider $r+1$ bits around the bipartite cut. Bits that are 0 prevent the corresponding bond term to appear in (4). Therefore, we just have to count the number of such bit strings that have for each pair of bits (one

from A, one from B) at distance smaller than r at least one bit set to 0. This is obtained by a series of $r-1$ bits set to 0 followed 1 at each end, e.g., for $r=4$ one has $\dots 10001 \dots$, and because we can put a cut at r different positions between these $r+1$ highlighted bits, we immediately get $a_r = r2^{L-r-1}$ ($L-r-1$ non-highlighted bits can have arbitrary values because they contribute to sub-leading terms). This holds as long as we are away from boundaries, that is $r \leq L/2$. Taking into account also boundaries one arrives at $a_r = r2^{L-r-1}$ if $r \leq L/2$, while $a_r = (r-2(r-\frac{L}{2}))2^{L-r-1}$ otherwise. As an example, for $L=4$ we have $a_1=4$, $a_2=4$ and $a_3=1$ (compare with the explicit (5)). For small ξ we can therefore write

$$\langle I(t) \rangle \approx \frac{2}{2^{L/2}} + \sum_{r=1}^{L-1} \frac{a_r}{N} e^{-\tau^2 W_r^2}. \quad (7)$$

For finite L the terms with $a_{r \leq L/2}$ will contribute in the first half (in logarithmic scale) of the decay to the asymptotic saturation, while smaller terms $a_{r > L/2}$ kick in only in the second half. As we are interested in the behavior in the thermodynamic limit we can safely make the limit $L \rightarrow \infty$ for each fixed t , obtaining purity decay in the thermodynamic limit and small ξ ,

$$\langle I(\tau) \rangle \approx \sum_{r=1}^{\infty} \frac{r}{2^{r+1}} e^{-\tau^2 W_r^2}, \quad (8)$$

where we abbreviated $\tau := Jt\sqrt{8}$, and we recall $W_r = e^{-(r-1)/\xi}$. For small ξ the values of W_r greatly differ for different r and so it follows that $\langle I(t) \rangle$ decays (and S_2 grows) in a series of steps (see Fig.1) connecting plateaus in purity. The value of the r -th plateau is at $I_r = 1 - \sum_{m=1}^r \frac{m}{2^{m+1}} = \frac{r+2}{2^{r+1}}$ (e.g., $I_r = \frac{3}{4}, \frac{4}{8}, \frac{5}{16}, \dots$ for $r = 1, 2, 3, \dots$). The sum in (8) still obscures the time dependence of $I(t)$. To get a better understanding we study at what times different plateaus are reached. The transition from one to the next plateau happens when

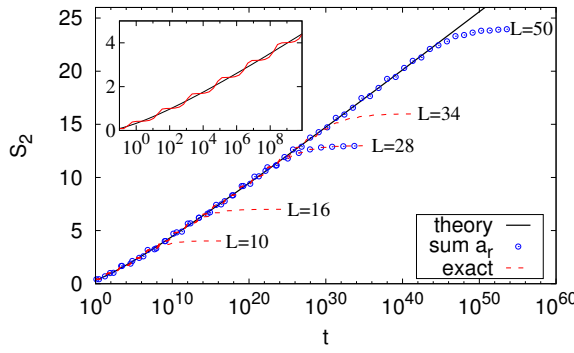


FIG. 1. (Color online) Entanglement growth in a 2-body random dephasing model for small localization length $\xi = 0.25$, $S_2 = -\log_2 I(t)$. Full curve is Eq. (9), circles the sum (7) and red curves the exact Eq. (4). The inset shows a small time zoom-in, showing plateaus.

the argument $\tau_r^2 W_r^2 \approx 1$, that is at a time satisfying $r-1 \approx \xi \ln \tau_r$, at which the value of $-\log_2 \langle I(t) \rangle$ is around $\frac{1}{2}(-\log_2 I_{r-1} - \log_2 I_r) \approx r + \frac{1}{2} - \log_2(r + \frac{3}{2})$. Putting the two together results in (expression is expected to be valid for large r , i.e., large $\xi \ln \tau$)

$$S_2(\tau) \approx \xi \ln \tau + A(\xi) - \log_2 [B(\xi) + \xi \ln \tau], \quad (9)$$

with $A(\xi) = \frac{3}{2}$, $B(\xi) = \frac{5}{2}$. We keep an explicit dependence of A, B on ξ because, as we shall show, the same form with a ξ -dependent constants is obtained also at larger ξ . Eq.(9), showing that entanglement does not grow as a simple logarithm of time, is our main result. While the leading logarithmic dependence has been observed and heuristically explained before, we also get a new negative logarithmic correction $\log_2 [B(\xi) + \xi \ln \tau]$.

Taking instead of the mean plateau either I_{r-1} or I_r we get a lower/upper bound on $-\log_2 \langle I(t) \rangle$ for which $A(\xi) = 1$ (2) and $B(\xi) = 2$ (3) for the lower (upper) bound. From the derivation it is clear from where does the log-log correction come: it is due to the numerator r in Eq.(8) which is in turn related to the linear growth of the number of different possible connections of length r crossing the cut. It is therefore a robust feature independent of a particular 2-body model (the denominator 2^{r+1} on the other hand comes from the Hilbert space size of all states connected with bonds of length $\leq r$).

One can also give an alternative analytic derivation of the logarithmic correction. Replacing the sum in Eq.(8) with an integral over r , in turn changing the variable r to $y := \tau^2 e^{-2(r-1)/\xi}$, one gets

$$\langle I(\tau) \rangle \approx \frac{\xi}{8} 2^{-\xi \ln \tau} \int_0^{\tau^2} \frac{1 + \xi \ln \tau - \frac{\xi}{2} \ln y}{y^{1-\frac{\xi}{2} \ln 2}} e^{-y} dy. \quad (10)$$

This integral is very handy for deriving the asymptotic expansion valid for $\xi \ln \tau \gg 1$. Namely, at the upper limit of integration the argument of the integral is exponentially small and we can safely extend the upper limit of integration to infinity. The resulting integral is elementary

end equal to $\Gamma(\frac{\xi}{2} \ln 2) \left(1 + \xi \ln \tau - \frac{\xi}{2} \Psi(\frac{\xi}{2} \ln 2)\right)$, where $\Gamma(z)$ is the Gamma function and $\Psi(z) := \Gamma'(z)/\Gamma(z)$ the Digamma function. Taking a negative logarithm of purity to get S_2 the expression has the same form as in Eq.(9), with

$$A(\xi) = -\log_2 \left[\frac{\xi}{8} \Gamma \left(\frac{\xi}{2} \ln 2 \right) \right], \quad B(\xi) = 1 - \frac{\xi}{2} \Psi \left(\frac{\xi}{2} \ln 2 \right). \quad (11)$$

Compared to the values of A and B obtained from the plateau analysis we here also have a ξ -dependent corrections (B can also be expressed as $B(\xi) = \xi \frac{dA(\xi)}{d\xi} + 1 + 1/\ln 2$), with the limiting values $A(\xi \rightarrow 0) \approx 1.47$ and $B(\xi \rightarrow 0) \approx 2.44$, see Fig. 2. In Fig. 1 we show comparison of the exact $S_2(t)$ (4), the approximate sum (7), and analytic result Eq.(9) with $A(0.25) \approx 1.53$ and $B(0.25) \approx 2.50$ obtained from Eq.(11). Excellent agreement is observed.

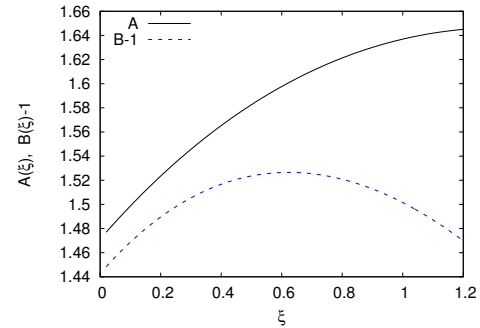


FIG. 2. (Color online) Dependence of $A(\xi)$ and $B(\xi)$ in Eq.(9) for small localization length ξ as given by Eq. (11).

B. Larger localization length

At larger ξ one has to take into account also the sub-leading terms W_p^2 in the argument of the exponential (4); neglecting them as in Eq.(8) gives a rigorous upper bound on purity. One can also get a (poor) lower bound on $I(t)$ by replacing all subleading terms with the leading W_r^2 , such that the argument of the exponential is at most $\tau^2(L^2 - r^2)W_r^2$, again resulting in a bound with a logarithmic correction. To get a better estimate we write a sum $\sum_{p=r}^{L-1} c_{m,p}^{(r)} W_p^2$ in (6) in terms of a prefactor x (that can in principle depend on r) as $\sum_{p=r}^{L-1} c_{m,p}^{(r)} W_p^2 =: (1+x)W_r^2$. We want to account for different x statistically, describing it by a probability distribution $p(x)$. One can get the exact expression for the average \bar{x} by averaging over all a_r arguments of the exponential function in Eq.(6), $\frac{1}{a_r} \sum_{m,p} d_m c_{m,p}^{(r)} W_p^2 =: W_r^2(1 + \bar{x})$. Counting the number of times $w_p := \sum_m d_m c_{m,r+p}^{(r)}$ one gets each $W_{r+p > r}^2$ in the r -th order terms, one gets, by a similar argument as used for a_r , that $w_p = (p+3)r2^{L-r-3}$,

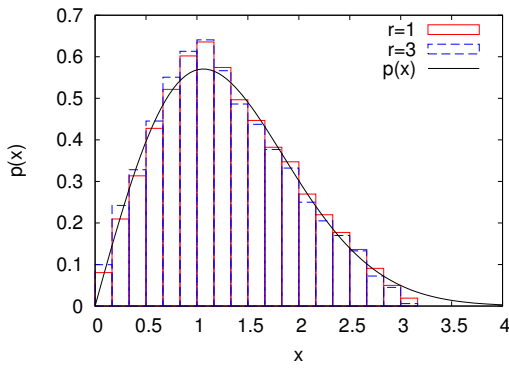


FIG. 3. (Color online) Distribution of x (see text for definition) for $L = 14$, $\xi = 3$, and $r = 1$ (distribution is over all $a_1 = 4096$ terms with $r = 1$), as well as $r = 3$ ($a_3 = 3072$). Full curve is heuristic $p(x)$ that we use (see text), with $b \approx 2.26$ determined from theoretical value of \bar{x} .

and as a consequence $1 + \bar{x} = 1 + \sum_{p=1}^{\infty} \frac{p+3}{4} e^{-2p/\xi} = \frac{1}{16}(3 + 1/\tanh(1/\xi))^2$ irrespective of r (in the TDL). The simplest improvement compared to the small- ξ result would be to replace τ in Eq.(9) with $\tau\sqrt{1 + \bar{x}}$, i.e., just rescaling time, which can in turn be absorbed in constants $A(\xi)$ and $B(\xi)$. One can do a bit better though. Looking at a numerical distribution $p(x)$ for intermediate ξ , such that finite size effects for our L are negligible, we find (Fig. 3) that $p(x) = \frac{2x}{b} e^{-x^2/b}$ describes the distribution reasonably well. Using $\bar{x} := \int_0^{\infty} p(x) x dx = \sqrt{\pi b/4}$ one can determine the needed b for each ξ such that \bar{x} has the required exact value. Averaging over such parameter-free $p(x)$ the purity can be written as

$$\langle I(t) \rangle = \int_0^{\infty} \frac{r+1}{2^{r+2}} e^{-\tau^2(1+x)} e^{-2r/\xi} \frac{2x}{b} e^{-x^2/b} dr dx. \quad (12)$$

The integral over r can be evaluated (it is the same as the infinite integral in Eq. (10) with a rescaled $\tau \rightarrow \tau\sqrt{1 + \bar{x}}$), obtaining

$$I(\tau) = \frac{\xi}{8} \Gamma\left(\frac{\xi}{2} \ln 2\right) \frac{1}{\tau^{\xi \ln 2}} \frac{1}{(1+x)^{\frac{\xi}{2} \ln 2}} \left[1 + \xi \ln \tau + \frac{\xi}{2} \ln(1+x) - \frac{\xi}{2} \Psi\left(\frac{\xi}{2} \ln 2\right) \right]. \quad (13)$$

Finally averaging this over $p(x)$ and taking the logarithm of the average in order to get S_2 , we again obtain the

familiar

$$\begin{aligned} S_2(\tau) &= \xi \ln \tau + A(\xi) - \log_2 [B(\xi) + \xi \ln \tau], \\ A(\xi) &= -\log_2 \left[\frac{\xi X_1}{8} \Gamma\left(\frac{\xi}{2} \ln 2\right) \right], \\ B(\xi) &= 1 - \frac{\xi}{2} \Psi\left(\frac{\xi}{2} \ln 2\right) + \frac{\xi X_2}{2X_1}, \\ X_1 &:= \int_0^{\infty} \frac{1}{(1+x)^{\frac{\xi}{2} \ln 2}} \frac{2x}{b} e^{-x^2/b} db, \\ X_2 &:= \int_0^{\infty} \frac{\ln(1+x)}{(1+x)^{\frac{\xi}{2} \ln 2}} \frac{2x}{b} e^{-x^2/b} db, \end{aligned} \quad (14)$$

where b is determined from ξ by $\sqrt{\pi b/4} = \frac{1}{16}(3 + 1/\tanh(1/\xi))^2 - 1$. The form that we get for S_2 is the same as in Eq.(9) with a modified $A(\xi)$ and $B(\xi)$ that are shown in Fig. 4. In Figs. 5 and 6 we show comparison

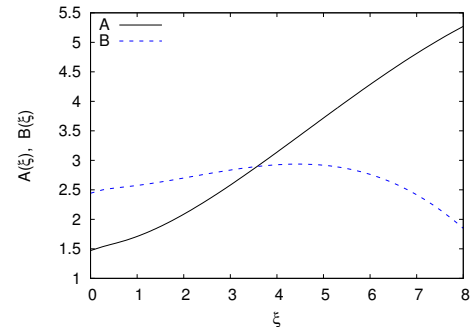


FIG. 4. (Color online) Dependence of $A(\xi)$ and $B(\xi)$ for larger ξ as given by Eq. (14).

between the exact S_2 and our approximate result (14), finding good agreement. Note that for larger ξ theoretical form Eq. (14) describes S_2 well for not too short times such that $S_2 \gtrsim \xi$. In order to clearly see the logarithmic correction we also show logarithmic derivative of S_2 (9) that behaves as $dS_2/d(\ln t) = \xi - \xi/[(B + \xi \ln \tau) \ln 2]$, that is, it approaches ξ as $\sim 1/\ln t$.

We have throughout focused on a particular initial state and distribution of couplings. We show in Appendix A that different generic initial product state, different distribution of coupling constants, as well as using von Neumann entropy, leads to essentially to same results as our exact calculation for a particular initial state and S_2 .

IV. THE 3-BODY RANDOM MODEL

A natural question is if any of the results obtained for the 2-body model, in particular the logarithmic correction, could be modified by higher r -body diagonal interactions (1), which, thou being less important (for an MBL phase $J^{(r)}$ should decay exponentially in r), could bring some fundamentally different behavior. As we explained, because the correction essentially comes from

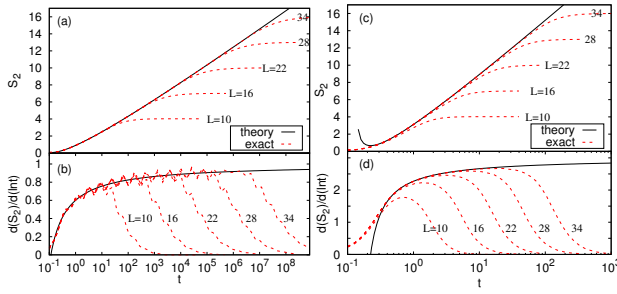


FIG. 5. (Color online) Entanglement growth in a 2-body random dephasing model for $\xi = 1$ in (a) and (b), and $\xi = 3$ in (c) and (d). (b) and (d) show logarithmic derivatives, clearly indicating the presence of a logarithmic correction (14). Theory here represent (14) with $A(1) \approx 1.71$, $B(1) \approx 2.57$, and $A(3) \approx 2.58$, $B(3) \approx 2.83$.

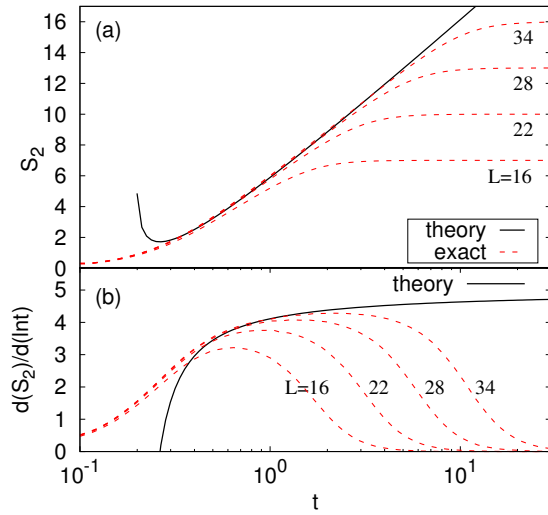


FIG. 6. (Color online) Same as Fig. 5 for $\xi = 5$, with $A(5) \approx 3.72$, $B(5) \approx 2.92$. Agreement with the theory (14) starts when $S_2 \gtrsim \xi$.

simple geometrical bonds counting, this is unlikely. In the following we present exact results demonstrating that.

To this end we consider a pure 3-body random model, where only $J_{k,l,m}^{(3)}$ are nonzero and i.i.d. Gaussian numbers with the variance $\langle J_{k,l,m}^{(3)} \rangle = J^2 W_r^2 = J^2 e^{-2(m-k-1)/\xi}$, where $k < l < m$. Taking the initial state that is a uniform mixture of all basis states, $c_{i\alpha} = 1/\sqrt{N}$, one gets

$$I(t) = \frac{1}{N^2} \sum_{\substack{i,j \in A \\ \alpha, \beta \in B}} \exp \left(-it \left[\sum_{\substack{l,m \in B \\ k \in A}} (z_k^i - z_k^j) J_{k,l,m}^{(3)} (z_l^\alpha z_m^\alpha - z_l^\beta z_m^\beta) + \sum_{\substack{k,l \in A \\ m \in B}} (z_k^i z_l^i - z_k^j z_l^j) J_{k,l,m}^{(3)} (z_m^\alpha - z_m^\beta) \right] \right). \quad (15)$$

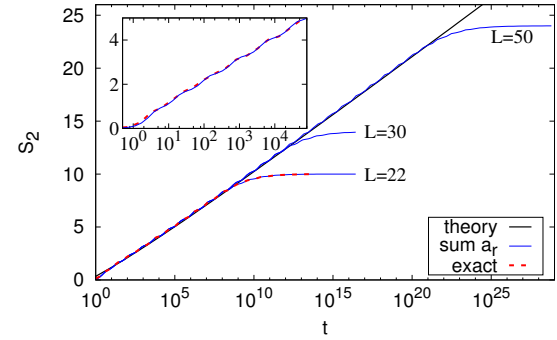


FIG. 7. (Color online) Random 3-body dephasing model for $\xi = 0.5$. Exact entanglement S_2 (red dashed curves) almost overlaps with the approximation (16) and with theory (17).

Compared to the 2-body model the saturation value has an exponentially small correction and is for an equal bipartite cut $L_A = L/2$ equal to $\overline{I}(t) = 2/2^{L/2}$. Averaging over Gaussian distribution of couplings we get a sum of Gaussian functions, like in (6), though with a more complicated combinatorics of c 's and d 's.

We shall focus on small ξ case where one can again neglect the subleading terms $W_{l>r}^2$. Counting the number of terms with the leading order r one gets $a_r = (r2^r + 6)2^{L-2r-1} = r2^{L-r-1}(1 + \frac{6}{r2^r})$, for $r = 2, \dots, L/2$, and $a_r = (L-r)2^{L-r-1}$ otherwise (note that for the 3-body model the smallest distance is $r = 2$). Therefore, asymptotically for large r the form of a_r is the same as for the 2-body model. What is different though is that the leading prefactor $c_{m,r}^{(r)}$ is not 1. Some of the a_r terms have a prefactor $c_{m,r}^{(r)} = r-1$, some $c_{m,r}^{(r)} = 2(r-1)$. The fraction of those with $c_{m,r}^{(r)} = r-1$ is equal to $\frac{2+r2^{r-1}}{3+r2^{r-1}}$ which goes to 1 for large r (for $r=2$ it is $\frac{6}{7}$). We shall therefore neglect terms with $c_{m,r}^{(r)} = 2(r-1)$, writing the average purity

$$\langle I(t) \rangle \approx \sum_{r=2}^{L-1} \frac{a_r}{2^L} e^{-(r-1)\tau^2 W_r^2} \asymp \sum_{r=2}^{\infty} \frac{r}{2^{r+1}} e^{-(r-1)\tau^2 W_r^2}. \quad (16)$$

Compared to the 2-body model the only difference is an additional factor $r-1$ in front of τ^2 . Calculating the time when $I(t)$ hits the middle between two consecutive plateaus, similarly as for the 2-body model, one gets $r \approx \xi \ln \tau_r + 1 + \frac{\xi}{\tau} \ln (\xi \ln \tau_r)$, resulting in

$$S_2(\tau) \approx y + \frac{3}{2} - \log_2 \left(y + \frac{5}{2} \right), \\ y := \xi \ln \left[\tau (\xi \ln \tau)^{p/2} \right], \quad (17)$$

where $p = 1$ for the 3-body model, coming from a $c_{m,r}^{(r)} = (r-1)^p$, while the 2-body small- ξ result (9) is obtained for $p = 0$. In terms of the scaling variable y the form is the same as for the 2-body model,

where the scaling variable was $y_{2\text{-b}} := \xi \ln \tau$. Expanding the logarithm we have $y = \xi \ln \tau + \frac{\xi}{2} \ln(\xi \ln \tau)$, and therefore, compared to the 2-body result (9), there is an additional logarithmic correction proportional to ξ . The same holds for any other finite p , and even after averaging over different p one would get at most $S_2 = u + A(\xi) + C(\xi) \ln u - \log_2 [u + B(\xi) + C(\xi) \ln u]$, where $u := \xi \ln \tau$. Therefore, we conjecture that any r -particle interaction (with finite r) can not fundamentally alter logarithmic corrections that we have found. One difference though worth mentioning is that for large ξ (or p) the positive prefactor $C(\xi)$ of the first correction can be larger than $1/\ln 2$ (a negative prefactor of the 2nd correction) and so in total the corrections can be positive instead of negative – entanglement growth is slightly faster than logarithmic. In the 2-body model it was always slightly slower.

V. MANY-BODY LOCALIZATION

So-far we have calculated the evolution of entanglement in the 1-bit basis, how about the original physical basis of an MBL system? For that one has to apply a basis rotation at $t = 0$, and at final t . Because it is a quasi-local unitary that transforms between the two bases, i.e., a finite-depth circuit [22], it can modify the entanglement S_2 only by a constant term that is proportional to the circuit depth/localization length. For long times when S_2 is large this can not modify neither the leading log term, nor the subleading correction because they all grow with time. In a realistic MBL system, unless the localization length is very small, many different r -body terms in H will contribute. While, as we argued, this will not change the form of the subleading correction, it will influence constants $A(\xi), B(\xi), C(\xi)$, as well as likely wash-out sharp plateaus in the growth that we observed for small localization length.

VI. SPECTRUM EVOLUTION

Full information about entanglement properties of a given pure state is contained in the spectrum λ_j of $\rho_A(t)$. While S_2 , being a scalar quantity that depends on eigenvalues λ_j , subsumes overall evolution of entanglement we here consider also dependence of each individual $\lambda_j(t)$, $j = 0, \dots, N_A - 1$, ordered nonincreasingly, $\lambda_j \geq \lambda_{j+1}$. Results of numerical simulation for the 2-body model are shown in Fig. 8 and 9. Looking at the time dependence of λ_j (Fig. 9a) we can see that they have a non-monotonic dependence (except the largest one λ_0 , data not shown), with a single maximum achieved at some t_{\max} , while at large time they approach λ_j for random states, given implicitly [44] by $2^{L/2} \lambda_j = 4 \cos^2 \varphi_j$, where $\frac{\pi}{2} \frac{j+0.5}{2^{L/2}} = \varphi_j - \frac{1}{2} \sin(2\varphi_j)$. These long-time values are the same as for evolution by completely random diagonal matrices [43]. Time t_{\max} strongly depends on j , i.e.,

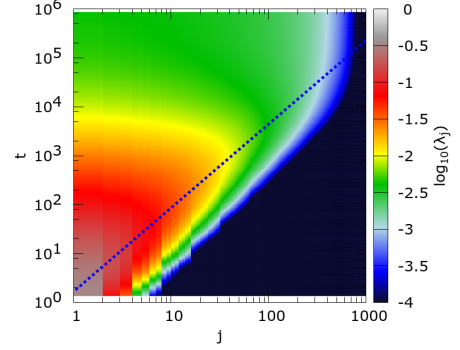


FIG. 8. (Color online) Time evolution of the reduced density matrix eigenvalues λ_j for a half-cut and the 2-body dephasing model with $\xi = 1$ and $L = 20$. Dashed blue line is (see also Fig. 9) $t_{\max} \approx 1.8j^{1.7}$, giving location of the maxima of $\lambda_j(t)$.

the larger eigenvalues “turn on” the fastest (which is different than in generic evolution modeled by a random matrix [45]), the dependence being $t_{\max}(j) \approx f(\xi) j^{1.7/\xi}$. The value at the maximum $\lambda_j(t_{\max}(j))$ is on the other hand $\sim 1/j$ and is independent of ξ and L (this is in line with a generic volume-law states reached at that late time). Therefore, correlations spread gradually from larger λ_j to smaller, in line with exponentially decaying couplings. We note that the power $1.7/\xi$ in $t_{\max} \sim j^{1.7/\xi}$ is smaller for larger ξ . It can be explained simply from the scaling of distance $r - 1 \sim \xi \ln t$, which relates to $j \sim 2^r$ eigenvalues being nonzero at that time. This results in a scaling $t \sim j^{1/(\xi \ln 2)}$. That the prefactor $1/\ln 2 \approx 1.44$ is not exactly 1.7 is because of certain arbitrariness in choosing the precise time that we look at. After time t_{\max} the eigenvalues gradually relax to their random-state asymptotic values. We end by noting that

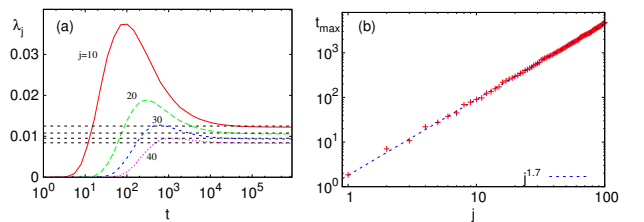


FIG. 9. (Color online) Same as in Fig. 8. (a) Few selected $\lambda_j(t)$ for $L = 16$. Horizontal lines are theoretical values (see text) for random states. (b) Location of the maxima for different j (time t_{\max} is independent of L ; we show $L = 20$, the same data as in Fig. 8).

the entanglement spectrum of eigenstates has proved to be useful for understanding MBL before [46], as well as the Schmidt gap [47] and the distribution of entanglement [48].

VII. CONCLUSION

We have calculated the exact form of entanglement evolution (within well controlled approximations) for a diagonal 1-bit model of many-body localization, showing that the “established” logarithmic growth is in fact not exact. This constitutes one of few analytical results for many-body localized systems. As such it should be valuable as a benchmark property of a widely accepted characterization of localization through correlations spreading. The techniques used can be generalized to more than one dimension. Finding a so-far unknown contribution shows the importance of pursuing exact calculations also for other quantities, thereby providing a more solid footing for the many-body localization against which results of numerical studies can be compared.

ACKNOWLEDGEMENTS

This work is supported by Grants No. J1-7279 and P1-0044 from the Slovenian Research Agency.

Appendix A: Numerical checks

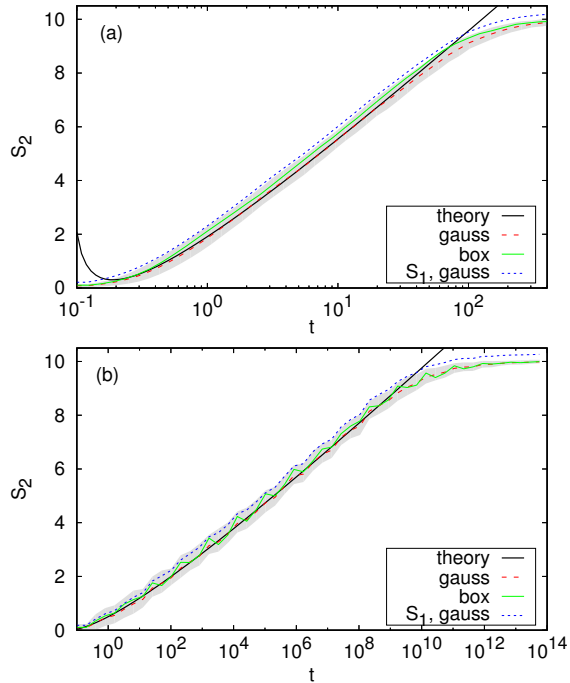


FIG. 10. (Color online) Comparison of S_2 for a Gaussian distribution of couplings and a box distribution (with the same variance). (a) is for $\xi = 2$, (b) for $\xi = 0.5$, both for $L = 22$. Theory is (14), gray shading denotes standard deviation of S_2 for a Gaussian case, while blue dotted curves show von Neumann entropy S_1 .

Here we verify that the physics of entanglement growth

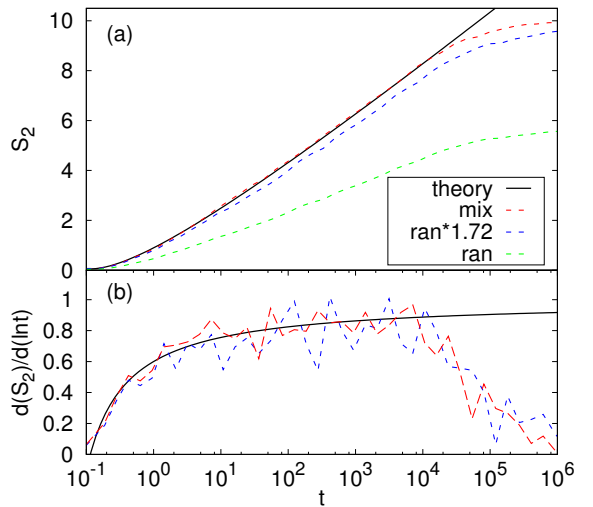


FIG. 11. (Color online) Comparison of S_2 (in (a)) and its derivative (in (b)) for a uniform mixture initial state, $c_{j\alpha} = 1/\sqrt{N}$ (red dashed curve, labeled “mix”), and random product states on the Bloch sphere (labeled “ran”, blue and green curve), all for $L = 22$ and $\xi = 1$. Blue dashed curve is data for the green one multiplied by 1.72 $\approx (1 \cdot 11 - 1)/(0.62 \cdot 11 - 1)$.

in the 2-body model is essentially the same also for other distributions of $J^{(2)}$, other Reny entropies, and initial states that do not have simple $c_{j\alpha} = 1/\sqrt{N}$.

In Fig. 10 we compare numerically calculated S_2 for a Gaussian distribution of couplings that was discussed in the main text, and for which analytics is the simplest, and a box distribution. We can see that the behavior is essentially the same. For a non-Gaussian distribution in Eq.(6) one would for instance instead of a sum of Gaussian functions have a sum of Fourier transformations of the distribution. For the box distribution and small ξ (e.g., frame (b) in Fig. 10) one can see a non-monotonic increase of S_2 that is due to oscillating nature of the Fourier transformation of the box distribution – any distribution with a finite support will exhibit such diffractive oscillations. We can also see that, as anticipated, the relative variance $\sigma(S_2)/S_2$ goes to zero for large times. Volume-law states that appear at late times are self-averaging and one can replace the average of the logarithm with a logarithm of the average, as we have done throughout. Last point to note in Fig. 10 is that the von Neumann entropy, denoted by S_1 , behaves similarly as S_2 .

We also check different initial states. We argued that the choice $c_{j\alpha} = 1/\sqrt{N}$ was mostly for analytical convenience and that other generic product initial state choices should result in the same entropy growth. From a finite-size effects point of view it is best to choose product initial states that have zero expectation of σ_j^z , $z = 0$, as this results in the largest saturation value $S_2(t \rightarrow \infty) = c \frac{L}{2} - 1$, where $c = \log_2 \frac{2}{1+z^2}$. As long as the initial state is a product state with all single-site orientations being in

the $x - y$ plane, the results presented are still exact after averaging over *i.i.d.* distribution of orientations within the $x - y$ plane. For initial states that have random uniform orientation on the Bloch sphere the saturation value will be smaller; it can be estimated by averaging c over the Bloch sphere, giving $\int_0^1 \log_2 \frac{2}{1+z^2} dz = \frac{4-\pi}{\ln 4} \approx 0.62$.

In Fig. 11 we compare data for a random product initial state and a state with $c_{j\alpha} = 1/\sqrt{N}$, seeing that after we rescale the random data by a theoretical factor accounting for different asymptotic saturation values, the two behave essentially the same, including the logarithmic correction (frame (b)).

[1] P. W. Anderson, Phys. Rev. **109**, 1492 (1958).
[2] D. M. Basko, I. L. Aleiner, and B. L. Altshuler, Ann. Phys. **321**, 1126 (2006).
[3] I. Gornyi, A. Mirlin, and D. Polyakov, Phys. Rev. Lett. **95**, 206603 (2005).
[4] V. Oganesyan and D. A. Huse, Phys. Rev. B **75**, 155111 (2007).
[5] M. Žnidarič, T. Prosen, and P. Prelovšek, Phys. Rev. B **77**, 064426 (2008).
[6] C. Monthus and T. Garel, Phys. Rev. B **81**, 134202 (2010).
[7] A. Pal and D. A. Huse, Phys. Rev. B **82**, 174411 (2010).
[8] R. Nandkishore and D. A. Huse, Annu. Rev. Condens. Matter Phys., **6**, 15 (2015).
[9] J. H. Bardarson, F. Pollmann, and J. E. Moore, Phys. Rev. Lett. **109**, 017202 (2012).
[10] M. Serbyn, Z. Papić, and D. A. Abanin, Phys. Rev. Lett. **110**, 260601 (2013).
[11] R. Vosk and E. Altman, Phys. Rev. Lett. **110**, 067204 (2013).
[12] I. H. Kim, A. Chandran, and D. A. Abanin, preprint [arXiv:1412.3073](https://arxiv.org/abs/1412.3073) (2014).
[13] M. Serbyn, Z. Papić, and D. A. Abanin, Phys. Rev. B **90**, 174302 (2014).
[14] D. A. Huse, R. Nandkishore, and V. Oganesyan, Phys. Rev. B **90**, 174202 (2014).
[15] A. Nanduri, H. Kim, and D. A. Huse, Phys. Rev. B **90**, 064201 (2014).
[16] A. Chandran, I. H. Kim, G. Vidal, and D. A. Abanin, Phys. Rev. B, **91**, 085425 (2015).
[17] V. Ros, M. Mueller, and A. Scardicchio, Nucl. Phys. B **891**, 420 (2015).
[18] J. Z. Imbrie, J. Stat. Phys. **163**, 998 (2016).
[19] J. Z. Imbrie, V. Ros, and A. Scardicchio, Ann. Phys. (Berlin) **529**, 1600278 (2017).
[20] M. Friesdorf et al., Phys. Rev. Lett. **114**, 170505 (2015).
[21] M. Friesdorf et al., New J. Phys. **17**, 113054 (2015).
[22] B. Bauer and C. Nayak, J. Stat. Mech. (2013) P09005.
[23] R. Vosk, D. A. Huse, and E. Altman, Phys. Rev. X **5**, 031032 (2015).
[24] J. Goold et al., Phys. Rev. B **92**, 180202(R) (2015).
[25] M. Serbyn, Z. Papić, and D. A. Abanin, Phys. Rev. X **5**, 041047 (2015).
[26] D. J. Luitz, N. Laflorencie, and F. Alet, Phys. Rev. B **93**, 060201 (2016).
[27] S. Bera and A. Lakshminarayan, Phys. Rev. B **93**, 134204 (2016).
[28] F. Iemini et al., Phys. Rev. B **94**, 214206 (2016).
[29] D.-L. Deng et al., Phys. Rev. B **95**, 024202 (2017).
[30] G. De Tomasi, S. Bera, J. H. Bardarson, and F. Pollman, Phys. Rev. Lett. **118**, 016804 (2017).
[31] M. Pino, Phys. Rev. B **90**, 174204 (2014).
[32] R. Singh, R. Moessner, and D. Roy, Phys. Rev. B **95**, 094205 (2017).
[33] P. T. Dumitrescu, R. Vasseur, and A. C. Potter, Phys. Rev. Lett. **120**, 070602 (2018).
[34] Y. Zhao, F. Andraschko, and J. Sirker, Phys. Rev. B **93**, 205146 (2016).
[35] M. J. Bremner, R. Jozsa, and D. J. Shepherd, Proc. R. Soc. A **467**, 459 (2011).
[36] We remark that the logarithmic growth of entanglement can not be used as a sole indicator of MBL. There are systems that display logarithmic complexity growth but are not MBL, e.g., non-interacting systems [37] with bond disorder [38] or long-range hopping [32], or even clean systems [39, 40]; there are also systems without an explicit disorder that have slow double-logarithmic growth [41].
[37] L. Hackl, E. Bianchi, R. Modak, and M. Rigol, preprint [arXiv:1710.04279](https://arxiv.org/abs/1710.04279) (2017).
[38] G. D. Chiara, S. Montangero, P. Calabrese, and R. Fazio, J. Stat. Mech. Theory Exp. (2006) P03001.
[39] N. Y. Yao et al., Phys. Rev. Lett. **117**, 240601 (2016).
[40] A. A. Michailidis et al., preprint [arXiv:1706.05026](https://arxiv.org/abs/1706.05026) (2017).
[41] M. Brenes, M. Dalmonte, M. Heyl, and A. Scardicchio, Phys. Rev. Lett. **120**, 030601 (2018).
[42] Y. Nakata, P. S. Turner, and M. Murao, Phys. Rev. A **86**, 012301 (2012).
[43] A. Lakshminarayan, Z. Puchala, and K. Žyczkowski, Phys. Rev. A **90**, 032303 (2014).
[44] M. Žnidarič, J. Phys. A: Math. Theor. **40**, F105 (2007).
[45] Vinayak and M. Žnidarič, J. Phys. A: Math. Theor. **45**, 125204 (2012).
[46] M. Serbyn, A. Michailidis, D. A. Abanin, and Z. Papić, Phys. Rev. Lett. **117**, 160601 (2016).
[47] J. Gray, S. Bose, and A. Bayat, preprint [arXiv:1704.00738](https://arxiv.org/abs/1704.00738) (2017).
[48] R. Singh, J. H. Bardarson, and F. Pollman, New J. Phys. **18**, 023046 (2016).